Research Square

Preprints are preliminary reports that have not undergone peer review.
They should not be considered conclusive, used to inform clinical practice,
or referenced by the media as validated information.

Thymosin alpha-1 Protected T Cells from Excessive Activation in Severe COVID-19

Kuai Yu
Sun Yat-sen University Cancer Center
Yongjian Wu
Sun Yat-sen University
Jingjing He
Sun Yat-sen University Cancer Center
Xuefei Liu
Sun Yat-sen University Cancer Center
Bo Wei
The Second Affiliated Hospital of Naval Military Medical University
Wen Wen
Fuzhou General Hospital of Fujian Medical University
Xiaofeng Wen
Sun Yat-sen University
Wenxiong Xu
the Third Affiliated Hospital of Sun Yat-sen University
Xingjun Dong
Sun Yat-sen University Cancer Center
Yue Yan
Sun Yat-sen University Cancer Center
Shuo Li
Sun Yat-sen University Cancer Center
Shuangye Liao
Sun Yat-sen University Cancer Center
Chenqi Gao
Sun Yat-sen University Cancer Center
Bei Zhong
The Sixth Affiliated Hospital of Guangzhou Medical University
Yongliang Jiang
The Sixth Affiliated Hospital of Guangzhou Medical University
Min Li
The Sixth Affiliated Hospital of Guangzhou Medical University
Chaochao Bian

Guangzhou FineImmune Biotechnology Co., LTD
Xiang Li
Guangzhou FineImmune Biotechnology Co., LTD
You Li
Guangzhou FineImmune Biotechnology Co., LTD
Haiping Liu
Guangzhou FineImmune Biotechnology Co., LTD
Xiangqi Chen
Fujian Medical University
Qingyu Zhao
Sun Yat-sen University Cancer Center
Xiaojun Xia
Sun Yat-sen University Cancer Center
Juanran Liang
Sun Yat-sen University
Bin Zou
Sun Yat-sen University
Bingliang Lin（✉ linbingl@mail.sysu.edu.cn）
the Third Affiliated Hospital of Sun Yat-sen University
Baosong Xie（✉ xbaosong@126.com）
Fujian Medical University
Lai Wei（✉ weil9@mail.sysu.edu.cn）
Sun Yat-sen University
Zhixiang Zuo（✉ zuozhx@sysucc.org.cn）
Sun Yat-sen University Cancer Center
Haibo Zhou（✉ haibo_zhou2003@163.com）
The Sixth Affiliated Hospital of Guangzhou Medical University
Xi Huang（✉ huangxi6@mail.sysu.edu.cn）
Sun Yat-sen University
Penghui Zhou（✉ zhouph@sysucc.org.cn）
Sun Yat-sen University Cancer Center

Research Article

Keywords: COVID-19, PBMCs, adaptive immune responses, lymphocyte phenotype, single-cell RNA sequencing

Posted Date: May 1st, 2020

DOI: https://doi.org/10.21203/rs.3.rs-25869/v1

License: This work is licensed under a Creative Commons Attribution 4.0 International License.
Read Full License

Version of Record: A version of this preprint was published on August 5th, 2020. See the published version at https://doi.org/10.1038/s41422-020-0391-9.

Abstract

Two typical features of uncontrolled inflammation, cytokine storm and lymphopenia, are associated with the severity of coronavirus disease 2019 (COVID-19), demonstrating that both innate and adaptive immune responses are involved in the development of this disease. Recent studies have explored the contribution of innate immune cells to the pathogenesis of the infection. However, the impact of adaptive immunity on this disease remains unknown. In order to clarify the role of adaptive immune response in COVID-19, we characterized the phenotypes of lymphocytes in PBMCs from patients at different disease stages using single-cell RNA sequencing (scRNA-seq) technology. Dynamics of the effector cell levels in lymphocytes revealed dysregulated adaptive immune responses in patients with severe disease. A new cluster of excessively activated CD8 T cells (Tea) was further identified, which displayed exhausted phenotypes and diminished function of antigen recognition. Interestingly, expression of PTMA, the proprotein of Tα1, was significantly increased in a group of highly proliferating CD8 T cells with memory stem cell features. We further showed that Tα1 significantly promoted the proliferation of activated T cells *in vitro* and relieved the lymphopenia in COVID-19 patients. Our data suggest that protection of T cells from excessive activation might be critical for the prevention of severe COVID-19.

Introduction

The outcome of a viral infection is mainly determined by the host immune system which is consisted of innate and adaptive immune cells. Appropriate immune responses eliminate invading viruses and establish immune memory for future protection[1]. However, an uncontrolled immune response may lead to severe immunopathology[2]. The SARS-CoV-2-caused coronavirus disease is characterized by uncontrolled inflammation, which may be similar to diseases resulted from the infections of other pathogenic coronaviruses such as the severe acute respiratory syndrome coronavirus-1 (SARS-CoV-1) and the Middle East respiratory syndrome coronavirus (MERS-CoV)[3-5]. Recent studies have focused on the mechanisms of innate immune response in this disease and clinical trials of therapies reducing inflammatory cytokines were thereby quickly initiated[6-8]. However, there is limited understanding on the role of the adaptive immunity in COVID-19. Deficiencies of adaptive immunity may not only impair the elimination of the infecting viruses but also lose the surveillance on other pathogens, which may lead to exacerbated infections and complicating diseases such as bacterial infections[9,10]. On the other side, a strong humoral immune response could lead to antibody-dependent enhancement (ADE) of viral infection[11-14]. Therefore, understanding of the adaptive immune responses in this disease may provide critical information for improving the treatment of COVID-19.

Results

Elderly patients have a high risk of Lymphopenia.

A high rate of severe COVID-19 was reported in immunocompromised patients, suggesting an insufficient rather than an overactive antiviral immunity could be the basis for the development of this disease[3,15].

Meanwhile, Lymphopenia, a reduction in the number of lymphocytes in the blood, was associated with the disease severity of COVID-19[3,16]. We analyzed the incidence of lymphopenia in 284 patients infected with SARS-CoV-2 collected from designated hospitals in Fujian province of China (basic information of the patients was listed in Table S1), and found that a reduction of lymphocytes was more frequently observed in aged patients (Fig. 1a). These findings denote the pivotal role of the adaptive immunity for the viral clearance and disease control.

scRNA-seq analysis identified main clusters in lymphocyte.

We hypothesized that single-cell transcriptomic analysis of peripheral lymphocytes during the course of the disease might clarify the role of the adaptive immune system in this disease. Therefore 13 samples of peripheral blood mononuclear cells (PBMCs) were collected from 10 patients at different stages of the disease, namely pre-severe disease (PR, 1 sample), severe disease (SD, 3 samples), post severe disease (PS, 3 samples), post mild disease (PM, 3 samples) and convalescence of mild disease (CM, 3 samples), which also included seven samples from our previous report (samples without enough number of lymphocytes were not included)[7]. Among all enrolled patients, four of them experienced severe disease under intensive care and the other six showed fever, cough, chill, and fatigue etc mild symptoms. Results of COVID-19 examination and times of sample collection were shown in Fig. 1b. Patient information was listed in Table S1. Samples of PM were collected from patients during hospitalization whose viral testing turned negative after treatment. Convalescent samples were collected within the first 5 days after hospital discharge. Three normal PBMCs from healthy donors (HD) were used as controls (named HD-1, HD-2, and HD-3).

We performed single-cell mRNA sequencing (scRNA-seq) of these samples on the 10x genomics platform. 243 million RNA transcripts in 91,649 cells were obtained after filtering cells with low quality. We then used t-Distributed Stochastic Neighbor Embedding (t-SNE) to visualize the clusters of all the cells identified by a shared nearest neighbor (SNN) modularity optimization based clustering algorithm implemented in Seurat[17] (Fig. 1c). The three major groups of immune cells in PBMCs, namely myeloid, B and T cells were clearly identified by specific gene expression signatures (Fig. 1d). Classic lineage markers further confirmed the identities of these clusters (Fig. 1e). We then focused on adaptive immune cells, and grouped the lymphocytes into B cells, CD4 and CD8 T cells (Fig. 1f and S1a). Analysis of the lymphocyte composition at different disease stages revealed a significant reduction in T cells along with increase in B cells in SD and PS samples (Fig. 1h), which indicates the abnormal dynamics of adaptive immune cells in patients with severe disease.

Humoral and cellular immune responses in patients with severe disease.

Effector cells carry out the major functions of the adaptive immune system, and decide the efficacy of adaptive immunity against viral infection. We checked the distribution of effectors in the clusters of lymphocytes. Despite the small numbers of cells identified, the plasma cells were prominently grouped (Fig. 1f). The T effectors were identified by the expression of GZMB, an effective molecule specifically

expressed in activated T cells. As shown in Fig. 1g, most of the effector T cells were located in the CD8 cluster, while CD4 effectors were barely detected.

In order to examine changes of effectors in different types of adaptive immune cells, we performed separate cluster analysis on the B, CD4 and CD8 T cells. B cells were grouped into 4 major clusters, namely mature, memory, activated B cells and plasma cells (Fig. 2a, S1b and S1e). CD4 T cells consisted of naïve, memory, effector and regulatory T cell clusters (Fig. 2c and S1c), while clusters of naïve, memory, effector and mucosal-associated invariant T cells (MAIT) were found In CD8 T cells (Fig. 2e and S1d). We found that the levels of effectors in these cells displayed different dynamics during the disease. The frequency of effectors in B cells was significantly increased at the SD stage but substantially reduced at the PS stage (Fig. 2b). Among CD4 T cells, Low levels of effectors were observed in all of the samples except for the one from PR (Fig. 2d). Consistent with the above observation (Fig. 1g), a large portion of effectors was found in CD8 T cells (Fig. 2e), but a significant low level of CD8 effectors was found at the PS stage (Fig. 2f).

Next, we examined changes of effectors in the humoral and cellular immune responses by measuring the frequencies of B (plasma cells plus activated B cells) and T effectors (CD4 plus CD8 effectors) in total lymphocytes respectively. In consistent with the observation in B cells, high levels of B effectors were observed in lymphocytes at the SD stage (Fig. 2g). For T effectors, however, low frequencies were found in lymphocytes at both the SD and PS stages (Fig. 2h), which was different from the observation in CD8 T cells among which low levels of effectors were only observed at the PS stage (Fig. 2f), This could be explained by the reduced portion of total T cells in lymphocytes at these two stages (Fig. 1h). Taken together, the dynamics of effector levels in lymphocytes revealed a coincidence of high humoral and low cellular immune responses at the stage of SD, which likely contributes to the progression of severe COVID-19.

Excessive activation led to exhaustion of CD8 T effector cells in sever COVID-19.

In order to understand the reduction of effector cells, we increased the modularity to group more distinct subsets, which allow us to explore the changes inside the major clusters. In CD8 T cells, two naïve, three memory and two effector clusters were identified after stringent grouping (Fig. 3a). No sub-clusters were detected in the MAIT cells. Gene expression signatures and pseudotime analysis demonstrated unbiased cellular dynamic processes of these sub-clusters (Fig. S2a and S2b). We then compared the two groups of effector T cells. Differentially expressed gene (DEG) and pathway enrichment analysis showed that one group was excessively activated, which was then named as Tea (excessively activate T cells). Compared to the normal effectors (Te), Tea cells had higher expression of activation genes (FCER1G, KLRB1, KLRF1, NKG7 and IGFBP7), co-inhibitory receptors (LAG3, CD300A, CD244, CD160 and HVCR2), IFN downstream signaling molecules (JAK1, IFITM2, IFITM3, TYK and IRF8), and chemokines (CCL3 and CCL5) (Fig. 3b and 3c). Significant reductions in TCR signaling molecules (CD3D, CD3G, CD8A, CD8B and ZNF683), and cytokine/receptor genes (IL7R, IL2RB, IL32 and IFNG) were found in Tea cells. For effector molecules, Tea cells expressed less GZMB but more PRF1 than Te cells. Although it is known that

activation induces cell death in T cells[18-21], we did not observe any significant difference in expression of apoptosis genes or pathways between these two clusters. This might have been due to the process of single cell analysis which excluded apoptotic cells to ensure the accuracy of clustering. Indeed, although the Tea cells expressed slightly more FAS and FASLG, both Tea and Te clusters expressed extremely low levels of these two genes (Fig. S2d). IFN signaling might be involved in the differentiation of Tea cells. Although CCL3 and CCL5 secreted by Tea cells may promote innate immunity, the slight increase of these two chemokines argued they were an effectual reservoir. As shown in Fig. 3d, CD8 effectors were dominated by Tea cells in SD samples, indicating that the adaptive immune system had been overwhelmed by these dysfunctional cells. Together, these data support that the Tea cells are a group of excessively activated T cells with exhausted phenotype and diminished function of antigen recognition. Excessive activation-induced continuous expansion of Tea cells may waste the majority of T cells, and lead to lymphopenia which paralyzes the adaptive immune system.

We then checked the CD8 memory T cells. The three sub-clusters were named as Tm-1, Tm-2 and Tm-3. Significant accumulation of Tm-3 was observed in the SD and PS stage (Fig. 3e), suggesting that this group of cells was specifically generated during severe disease. The percentage of Tm-3 in CD8 memory T cells was strongly correlated with the proportion of Tea in the CD8 effector cells (R^2=0.7813) (Fig. 3f), suggesting that Tm-3 might be a group of memory cells derived from the Tea cells during excessive activation. Differential gene expression analysis and pathway enrichment analysis showed that Tm-3 was a cluster of highly proliferating cells with features of memory stem cells (Fig. S2e and S2f). Compared to Tm-1 and Tm-2, Tm-3 had high expression of T memory stem cell markers (SELL, CXCR3, CCR7, FAS, CD27 and CD28), and the proliferation gene Ki67 (Fig. 3g)[22]. Furthermore, a slightly higher expression of GZMA and lower level of IL7R in the Tm-3, as compared to Tm-1 and Tm-2, also showed that this was a group of recently developed memory T cells. The low level of Tm-3 at the PR stage further confirmed its differentiation during severe disease stages (Fig. 3e).

Although both Tea and Tm-3 cells experienced excessive activation, exhaustion was observed in the Tea but not Tm-3 cells. We then performed DEG and pathway-enrichment analysis to understand the difference between these two groups of cells. The Tea cells had comparatively higher-level expression of T cell activation and effector genes (GNLY, NKG7 and GZMB) but almost had no expression of Ki67 (Fig. 3h and 3i), suggesting that they were end-differentiated cells and more prone to death. In contrast, the Tm-3 cells had high expression of genes involved in epigenetic modification (DNMT1 and EZH2), oxidative phosphorylation (NDUB6 and NDUFV2), regulation of telomerase, cell cycle and proliferation etc (Fig. 3h and 3i). These distinct signaling transduction and epigenetic changes might have shaped the stem-like memory phenotype of Tm-3. Interestingly, we found the expression of

Prothymosin alpha (PTMA) was also significantly increased in Tm-3 (Fig. 3h and 3j). Thymosin alpha-1 (Tα1), the first 28 amino acids of PTMA, was found to be involved in T cell development, and has been used for the treatment of certain infection diseases including COVID-19[23]. In addition, Tea expressed less PTMA than Te, and Tm-3 expressed the highest level of PTMA in all the sub-clusters of CD8 T cells (Fig. 3j). We thus suspected that Tα1 might protect T cells from excessive activation.

We further analyzed the subsets in naïve T cells but did not observed any significant change during the different disease stages (Data not shown). Since no sub-clusters were identified in the effector clusters of B cells and CD4 T cells, we did not analyze the subsets in these two types of adaptive immune cells (Data not shown).

Thymosin alpha-1 protected T cells from excessive activation.

Next, we tested the effect of Tα1 on T cell activation. PBMCs from healthy donors were activated by anti-CD3/CD28 antibodies *in vitro* and treated with 200ng/ml Tα1 for 3 days, followed by cultures with IL-2 (200U/ml) and Tα1 (200 ng/ml) for 6 more days. Compared to the control group, Tα1 had significantly increased T cell numbers at day 6 and 9 although a slightly decreased number in T cells was observed at day 3 (Fig. 4a), indicating that Tα1 promoted the proliferation of T cells after activation. After 3 days of activation, we found that cell size measured by FSC and SSC was slightly reduced in the group with Tα1 (Fig 4b), suggesting that these T cells were less activated. Tα1 treatment did not change the proportion of CD4 and CD8 T cells (Fig 4c), but reduced the production of IFNγ and TNFα, although no significant statistical difference was observed (Fig 4d). Significant reduction of granzyme B was observed in both CD4 and CD8 T cells, while no change in the expression of PD-1 was observed. These data showed that Tα1 could reduce T cell activation and promote the proliferation of T cells after activation, indicating it may protect the T cells from excessive activation.

The use of Tα1 in some COVID-19 patients may allow the evaluation of its impact on lymphocytes. The data from 25 severe and critical COVID-19 cases treated at the Huoshenshan hospital (Wuhan, China) were collected (basic information of the patients was listed in Table S1). Of them, 11 patients received daily Tα1 treatment for at least one week, while the other 14 patients were not treated with Tα1 during the hospitalization period. Compared to the non-treated patients, the lymphocyte counts of the treated patients were significantly increased after one week of Tα1 treatment (Fig. 4e). The fold change of lymphocytes counts in each patient was shown in Fig. 4f. These data showed that Tα1 enhanced the number of lymphocytes in patients with severe and critical disease. Due to the limited number of patients in this retrospective analysis, we were not able to clearly evaluate the clinical benefits of Tα1 treatment. Nevertheless, our data suggest that the administration of Tα1 could be a potential approach to protect T cells from excessive activation in COVID-19.

Discussion

The outbreak of the new coronavirus SARS-CoV-2 has resulted in a global pandemic. Due to the lack of a specific drug against this virus, the current clinical management of this disease mainly depends on supportive care to reduce inflammatory responses and to keep the lung functioning[24]. Understanding the underlying immunopathology of the COVID-19 is therefore of paramount importance for improving the current treatment. Our results revealed an unexpected elevation of effector B cells and the early absence of CD4 effector T cells in severely affected patients, while excessive activation-mediated exhaustion of CD8 T cells might be an important mechanism of lymphopenia founding patients with severe disease.

Our findings demonstrated that a disordered adaptive immune response may facilitate the infection of SARS-CoV-2 and thus cause the outbreak of severe disease, highlighting that the early protection of T cell from excessive activation may be a key step to prevent severe disease. Despite the promising preliminary results observed in Tα1 treated clinical patients, more novel therapies that are able to synergize with the patients' adaptive immune responses are needed in future. Enhanced activation-induced cell death has been reported in patients with advanced age[19]. Future evaluation of excessive activation in elderly patients may clarify if this is the cause for the high rate of severe disease observed in this group of patients. Since the Tea cells identified in this study could reflect the damage of the adaptive immunity, testing the portion of this group of cells in lymphocytes might serve a good prognostic marker to identify patients at high risk of developing severe disease.

Interestingly, the dynamics of B effector levels in lymphocytes observed in this study is similar to the reported antibody responses in patients infected with SARS-CoV-1, the virus caused the severe acute respiratory syndrome (SARS). High activities of neutralizing antibody were quickly developed but diminished rapidly later in deceased but not recovered SARS patients, who slowly developed these activities and maintained high levels for a long time[10,11,13]. In addition, recent reports also observed increased IgG and total antibody titer in severe COVID-19 patients, and found that high titer was associated with disease severity and worse outcome[12,14]. These findings suggested a possible role of ADE in COVID-19, which is a potential challenge for vaccine development, and needs to be further addressed.

Methods

Antibodies and reagents

The antibodies for flow cytometry were purchased from Biolegend or BD. Tα1 was purchased from ADAXIN. Chromium™ Single cell 5' Library & Gel Bead Kit (1000006), Chromium™ Single cell 3'/5' Library Construction Kit (1000020) was purchased from 10x Genomics. Cytokines were purchased from Peprotech. All cell culture reagents were purchased from Gibco unless otherwise indicated.

Patients and study approval

This study enrolled a total of 10 COVID-19 patients. The 4 patients with severe disease were reported in our previous study[7]. The 6 patients with mild disease (3 at post mild disease stage and 3 at convalescence stage) were recruited from the Fifth Affiliated Hospital (Zhuhai, China) and the Third Affiliated Hospital (Guangzhou, China) of Sun Yat-sen University. Lymphocyte count data from 25 SARS-CoV-2 patients were collected in Huoshenshan hospital (Wuhan, China) by managing doctors. Lymphocyte count data from 256 SARS-CoV-2 patients were collected from designated hospitals in Fujian province during January 3 2020 to march 13 by managing doctors. Informed consent has been obtained from all participated patients. This study received approval from the Research Ethics Committee

of the Sun Yat-sen University Cancer Center, the Fifth Affiliated Hospital, the Third Affiliated Hospital of Sun Yat-sen University, the Huoshenshan hospital and the Fujian Provincial Hospital, China.

PBMCs Isolation

All procedures were carried out within P2+ laboratory certified for studies of infectious materials. PBMCs were isolated from peripheral venous whole blood samples density gradient cell separation (Ficoll, TBD Science, China), and were preceded for Single cell transcriptome sequencing immediately.

Cell culture

Fresh PBMCs from healthy donors were cultured in IL-2 (200U/ml) containing media in 96-well u-bottomed plates coated with anti-CD3/CD28 (5ug/ml respectively, Peprotech). To test the effect on T cell activation, Tα1 (200ng/ml) was added into T cells culture media while seeding. Cell numbers were recorded at day 3, 6 and 9. Cells harvested after 3 days activation were analyzed by flow cytometry.

Flow cytometry

The antibodies used for cell surface labeling were BUV737 anti-human CD4 (564305, BD), BUV395 anti-human CD8 (563795, BD), FITC anti-human PD-1 (329904, Biolegend). The antibodies used for intracellular staining were PE anti-human IFNG (506507,Biolegend), APC anti-human TNFA (502912, Biolegend), BV421 anti-human Granzyme B (563389, BD). All antibodies for flow cytometry staining were used at 1:200 dilution. Cells were harvested and washed once in 2ml PBS and labeled on ice with indicated antibodies for analysis of surface markers. To determine intracellular cytokine expression, the cells were pre-incubated with Brefeldin A (Biolegend) for 4h before staining. After incubation, cells were stained following surface staining, fixation and permeabilization using the BD Transcription Factor Buffer Set (562574, BD) according to the manufacturer's instructions. All samples were analyzed on a LSRFortessa™ X-20 cell analyzer (BD Biosciences). Analysis of acquired data was performed with the FlowJo software (FlowJo LLC).

Single cell transcriptome sequencing and data preprocessing

The single cell RNA libraries were prepared using the Chromium^{TM} Single cell 5' Reagent Kit of Chromium platform (10x Genomics, USA) following the manufacturer's instruction. Generated single cell RNA libraries were sequenced on the Illumina HiSeq X Ten platform. The CellRanger software (version 3.1.0) was used for preprocessing of the PE150 Illumina sequencing reads. Briefly, raw reads in bcl format were converted to FASTQ format using "cellranger mkfastq", and then the reads in FASTQ format were aligned to human genome reference (hg38, GRCh38) using STAR, and then "cellranger count" was used to derive gene expression matrix for each sample.

Determination of cell types from single cell transcriptome sequencing data

Seurat (v3.1.3) R toolkit was used to analyze the single cell transcriptome sequencing data. Firstly, cells with low quality were filtered out. Briefly, the dead or dying cells with more than 20% mitochondrial RNA content were removed, and the cells with too low number (less than 200) or too high number (more than 2500) of genes were also removed, and the cells expressed more than one markers among the three markers (CD2, CD79A, CD68) were defined as doublets and removed. Then, the filtered gene expression matrix for each sample was normalized using “NormalizeData” function in Seurat, and only highly variable genes were remained using “FindVariableFeatures” function in Seurat. Next, “FindIntegrationAnchors” and “Integratedata” functions in Seurat were used to integrate the gene expression matrices of all samples, where batch effects between different samples have been adjusted. Next, “RunPCA” function was used to perform the principle component analysis (PCA) and “FindNeighbors” function was used to construct a K-nearest-neighbor graph. Next, the most representative principle components (PCs) selected based on PCA were used for clustering analysis with “FindCluster” function to determine different cell types. Lastly, tSNE was used to visualize the different cell types.

We annotated the cell types using the following three rules: 1) 20% cells with barcode detected by TCR or BCR can be defined as T cell or B cell. 2) Based on the most 10 differentially expressed genes that were derived using “FindAllMarkers” function in Seurat, genes such as CD2, CD3D, CD3E, and CD3G were used as T cell markers, and genes such as CD19, CD79A, CD79B, BLNK, FCRL5, MS4A1 were used as B cell markers, and genes such as CD14, CD163, CD68, CSF1R, FCGR2A, and CD33 were used as Myeloid cell mark. 3. The percentage of CD4 gene expression and CD8A was counted to define CD4+ T cells or CD8+ T cells.

The B cells, CD4 T cells and CD8 T cells were further clustered using the single cell analysis pipeline as described above. To get higher resolution clusters, the “resolution” parameter used in FindCluster was set from 0.3 to 0.5.

Differential gene expression analysis between different cell types

Seurat v3 was used to perform differential gene expression analysis between different cell types. For each cell type, the differentially expressed genes (DEGs) were obtained relative to all of the other cell types using “FindCluster” function in Seurat. DEGs between Tea cells and Te cells, and DEGs between Tm-3 and Tea were obtained using R package edgeR with log2 Fold change > 0.58 and *P* value < 0.5. Gene functional annotation For DEGs were performed using the R package clusterProfilter with default settings. The *P* values were corrected for multiple testing.

Single cell trajectories analysis

The R package Monocle 2 was used to analyze single cell trajectories in order to discover the cell-state transitions. We sampled 200 cells from each cell type and used genes with average expression > 0.1 to sort cells in pseudo-time order. “DDRTree” function in Monocle 2 was applied to reduce dimensions and “plot_cell_trajectory” function was used to visualize the minimum spanning tree on cells.

Statistical analysis.

All sample sizes were large enough to ensure proper statistical analysis. Statistical analyses were performed using GraphPad Prism (GraphPad Software, Inc.). P values < 0.05 were considered as statistically significant. All t-test analyses were one-tailed t-tests (paired or unpaired depending on the experiments). The number of replicates (n), number of independent experiments performed, and p values for each experiment are reported in the corresponding figure legends.

Declarations

Data Accession

The raw data files were deposited in the Genome Sequencing Archive of the National Genomics Data Center with the accession number of CRA002572. (https://bigd.big.ac.cn/search?dbId=&q=CRA002572)

Acknowledgement

We are indebted to the patients for their participation.

This study is supported by grants from the National Key Research and Development Program of China (no. 2016YFA0500304), the National Nature Science Foundation in China (NSFC) (81773052, 81572806), the Guangzhou Science Technology and Innovation Commission (201607020038), the Science and technology projects of Guangdong Province (2016A020215086), the Guangdong Innovative and Entrepreneurial Research Team Program (2016ZT06S638) the Medical Scientific Research Foundation of Guangdong Province (2016111214046444) and the leading talents of Guangdong province program.

Competing interests

P.Z. is a consultant and scientific founder of FineImmune; C.B., X.L., Y. L., H.L. are current employee of FineImmune. The other authors declare that they have no competing interests.

Author Contribution

P.Z. and L.W. conceived the study and drafted the manuscript; X.X. provided advices of experiments and edited the manuscript; K.Y., J.H., J.L., S.L., C.G., X.W., J.L. and B.Z. performed the scRNA sequencing experiments; C.B., X.L., Y.L. and H.L. performed second-generation sequencing; J.H., K.Y., Y.Y. and Q.Z. collected PBMCs from healthy donors and performed experiments of T cell activation. Z.Z., X.L., and X.D. performed data analysis; X.H., Y.W., W.X., B.Z., Y.J., M.L, H.Z. and B.L. supervised the collection of samples for scRNA sequencing; B.W. and S.L. collected and analyzed clinical data of Ta1 treatment. W.W., X.C. and B.X. supervised the collection and analysis of lymphocyte counts of COVID-19 patients. All authors read and approved the final version of the manuscript.

References

1. Fan, Y. *et al.* Characterization of SARS-CoV-specific memory T cells from recovered individuals 4 years after infection. *Arch Virol* **154**, 1093-1099, doi:10.1007/s00705-009-0409-6 (2009).
2. Cameron, M. J., Bermejo-Martin, J. , Danesh, A., Muller, M. P. & Kelvin, D. J. Human immunopathogenesis of severe acute respiratory syndrome (SARS). *Virus Res* **133**, 13-19, doi:10.1016/j.virusres.2007.02.014 (2008).
3. Wang, *et al.* Clinical Characteristics of 138 Hospitalized Patients With 2019 Novel Coronavirus-Infected Pneumonia in Wuhan, China. *JAMA*, doi:10.1001/jama.2020.1585 (2020).
4. Cao, X. COVID-19: immunopathology and its implications for therapy. *Nat Rev Immunol*, doi:10.1038/s41577-020-0308-3 (2020).
5. Li, X., Geng, M., Peng, , Meng, L. & Lu, S. Molecular immune pathogenesis and diagnosis of COVID-19. *J Pharm Anal*, doi:10.1016/j.jpha.2020.03.001 (2020).
6. Golonka, R. M. *et al.* Harnessing Innate Immunity to Eliminate SARS-CoV-2 and Ameliorate COVID-19 Disease. *Physiol Genomics*, doi:10.1152/physiolgenomics.00033.2020 (2020).
7. Wei, L. *et al.* Viral Invasion and Type I Interferon Response Characterize the Immunophenotypes during Covid-19 Infection. *SSRN Electronic Journal DOI: 10.2139/ssrn.3555695* (2020).
8. Tu, F. *et al.* A Review of SARS-CoV-2 and the Ongoing Clinical Trials. *Int J Mol Sci* **21**, doi:10.3390/ijms21072657 (2020).
9. Janice Oh, H. L., Ken-En Gan, S., Bertoletti, A. & Tan, J. Understanding the T cell immune response in SARS coronavirus infection. *Emerg Microbes Infect* **1**, e23, doi:10.1038/emi.2012.26 (2012).
10. Channappanavar, R., Zhao, J. & Perlman, S. T cell-mediated immune response to respiratory coronaviruses. *Immunol Res* **59**, 118-128, doi:10.1007/s12026-014-8534-z (2014).
11. Zhang, L. *et al.* Antibody responses against SARS coronavirus are correlated with disease outcome of infected individuals. *J Med Virol* **78**, 1-8, doi:10.1002/jmv.20499 (2006).
12. Zhao, J. *et al.* Antibody responses to SARS-CoV-2 in patients of novel coronavirus disease 2019. *Clin Infect Dis*, doi:10.1093/cid/ciaa344 (2020).
13. Liu, L. *et al.* Anti-spike IgG causes severe acute lung injury by skewing macrophage responses during acute SARS-CoV infection. *JCI Insight* **4**, doi:10.1172/jci.insight.123158 (2019).
14. Zhang, B. *et al.* Immune phenotyping based on neutrophil-to-lymphocyte ratio and IgG predicts disease severity and outcome for patients with COVID-19. *medRxiv preprint doi: https://doi.org/10.1101/2020.03.12.20035048.*, doi:10.1101/2020.03.12.20035048 (2020).
15. Chen, *et al.* Clinical characteristics and outcomes of older patients with coronavirus disease 2019 (COVID-19) in Wuhan, China (2019): a single-centered, retrospective study. *J Gerontol A Biol Sci Med Sci*, doi:10.1093/gerona/glaa089 (2020).
16. Tan, *et al.* Lymphopenia predicts disease severity of COVID-19: a descriptive and predictive study. *medRxiv preprint doi: https://doi.org/10.1101/2020.03.01.20029074*, doi:10.1101/2020.03.01.20029074 (2020).

17. Satija, R., Farrell, J. A., Gennert, , Schier, A. F. & Regev, A. Spatial reconstruction of single-cell gene expression data. *Nat Biotechnol* **33**, 495-502, doi:10.1038/nbt.3192 (2015).
18. Brenner, D., Golks, A., Kiefer, , Krammer, P. H. & Arnold, R. Activation or suppression of NFkappaB by HPK1 determines sensitivity to activation-induced cell death. *EMBO J* **24**, 4279-4290, doi:10.1038/sj.emboj.7600894 (2005).
19. Sikora, Activation-induced and damage-induced cell death in aging human T cells. *Mech Ageing Dev* **151**, 85-92, doi:10.1016/j.mad.2015.03.011 (2015).
20. Shin, S. , Kim, M. W., Cho, K. H. & Nguyen, L. K. Coupled feedback regulation of nuclear factor of activated T-cells (NFAT) modulates activation-induced cell death of T cells. *Sci Rep* **9**, 10637, doi:10.1038/s41598-019-46592-z (2019).
21. Krammer, H., Arnold, R. & Lavrik, I. N. Life and death in peripheral T cells. *Nat Rev Immunol* **7**, 532-542, doi:10.1038/nri2115 (2007).
22. Gattinoni, L., Speiser, D. , Lichterfeld, M. & Bonini, C. T memory stem cells in health and disease. *Nat Med* **23**, 18-27, doi:10.1038/nm.4241 (2017).
23. King, R. & Tuthill, C. Immune Modulation with Thymosin Alpha 1 *Vitam Horm* **102**, 151-178, doi:10.1016/bs.vh.2016.04.003 (2016).
24. Zhou, M., Zhang, X. & Qu, J. Coronavirus disease 2019 (COVID-19): a clinical update. *Front Med*, doi:10.1007/s11684-020-0767-8 (2020).

Supplemental Legends

Figure S1 The specific gene signatures of different immune cell types.

a. Heatmap showing differentially expressed genes between CD4, CD8, B cell and plasma. **b.** Heatmap showing differentially expressed genes between mature, memory, activated B cells and plasma cells. **c.** Heatmap showing differentially expressed genes between naive, memory, effector and regulatory CD4 T cells. **d.** Heatmap showing differentially expressed genes between naive, memory, effector CD8 T cells and mucosal-associated invariant T (MAIT) cells. **e.** Signature gene (IGHM, IGHG, IGHA, IGHD and IGHE) expression of B cells.

Figure S2 The specific gene signatures of CD8 T cell sub-clusters.

a. Heatmap showing differentially expressed genes between CD8 T cell sub-clusters. **b.** The order of CD8 T cells along pseudotime in a two-dimensional state-space defined by Moncle2. Each point corresponds to a single cell, and each color represents a cluster. **c.** The ridgeline plot visualizing the expression distributions of differentially expressed genes in Te and Tea cells. **d.** The ridgeline plot visualizing expression distributions of FAS and FSALG genes in Te and Tea cells. **e.** Heatmap showing differentially expressed genes between Tm-1, Tm-2 and Tm-3. **f.** Gene Ontology (GO) enrichment analysis of significantly differentially expressed genes between Tm-3 and Tea cells.

Figure S3 Gating strategy of FACS plots.

Table S1 Patient information

Table S1 was omitted by the authors in this version of the paper.

Figures

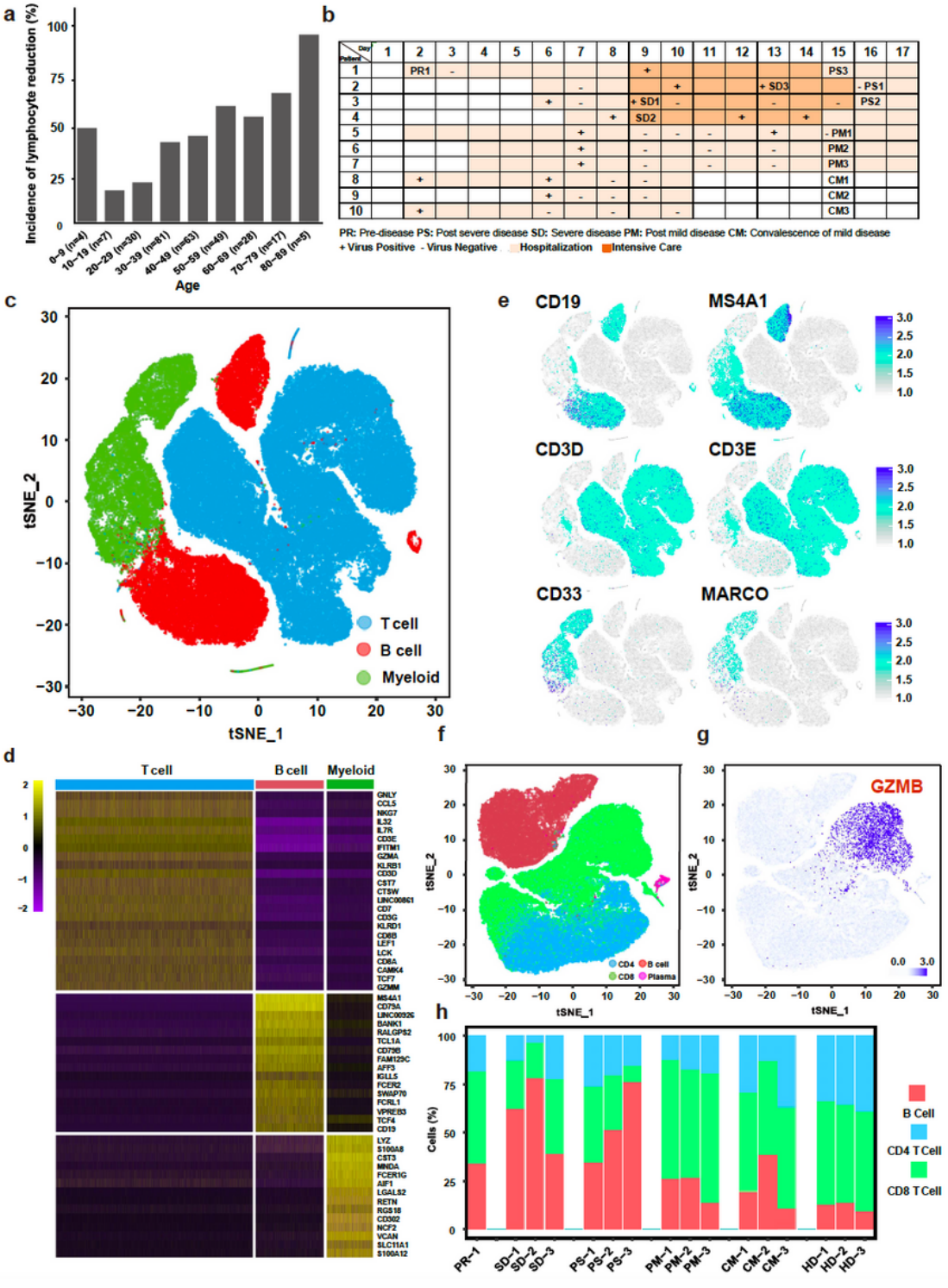

Figure 1

Lymphopenia in elderly patients and clusters of PBMCs. a. Bar plot showing the incidence of lymphocyte reduction in different age. b. Virus detection result and time of sample collection. c. The t-SNE projection of PBMCs from 10 patients and 3 healthy donors, showing the three main clusters including T cells (blue color), B cells (red color) and myeloid cells (green color). e. Heatmap showing differentially expressed genes between the three clusters. The top bar indicates cell types. d. The expression of selected T, B and myeloid cell markers in all the cells visualized in the t-SNE plot. e. The t-SNE projection of the lymphocyte cells, showing 4 sub-clusters including CD4 T cells (blue color), CD8 T cells (green color), B cells (red color) and Plasma cells (purple color). f. The expression of Effector T cell marker GZMB in all the lymphocyte cells. g. The proportion of CD4 T cells, CD8 T cells, and B cells in each patient.

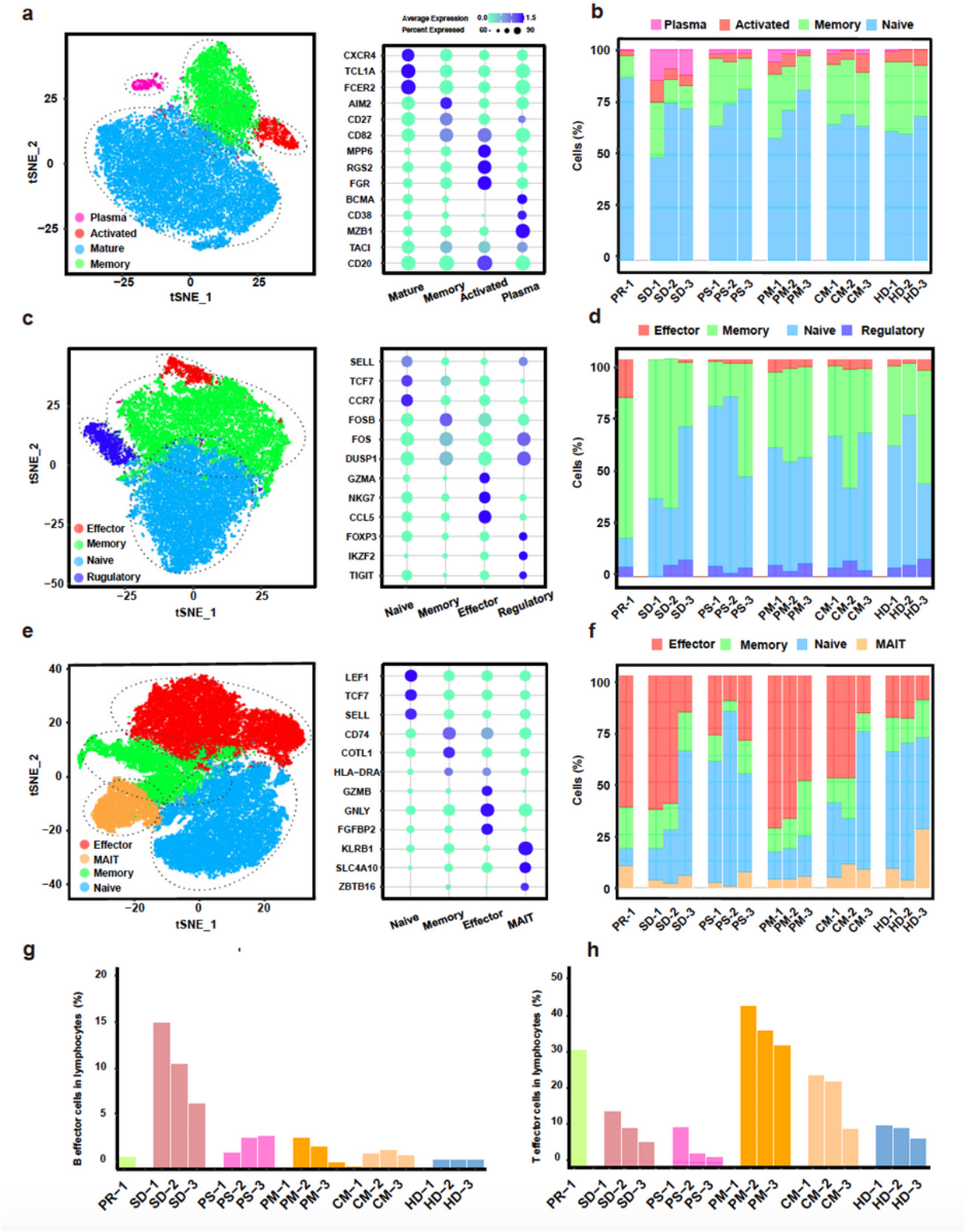

Figure 2

Dynamics of effector cells in the adaptive immune system. a. The t-SNE plot showing 4 main clusters of B cell including Plasma, activated, mature and memory B cells (left panel). Selected B cell markers are represented in the dot plot (right panel). The size of the dot represents the percentage of cells expressing the selected gene, and the color of dots represents average expression of the selected gene. b. The proportion of different B cells (Plasma, Activated, Memory, and Naïve) in each patient. c. The t-SNE plot

showing CD4 T cell clusters (left panel) and the dot plot showing the average expression and percentage of the selected genes in each cluster (right panel). d. The proportion of CD4 T cells (Effector, Memory, Naive, and Regulatory) in each patient. e. The t-SNE plot showing CD8 T cell clusters (left panel) and the dot plot showing the average expression and percentage of the selected genes in each cluster (right panel). f. The proportion of CD8 T cells (Effector, Memory, Naive, MAIT) in each patient. g. The bar plot showing the proportion of effector B cells in all lymphocytes in each patient. h. The bar plot showing the proportion of effector T cells in all lymphocytes in each patient.

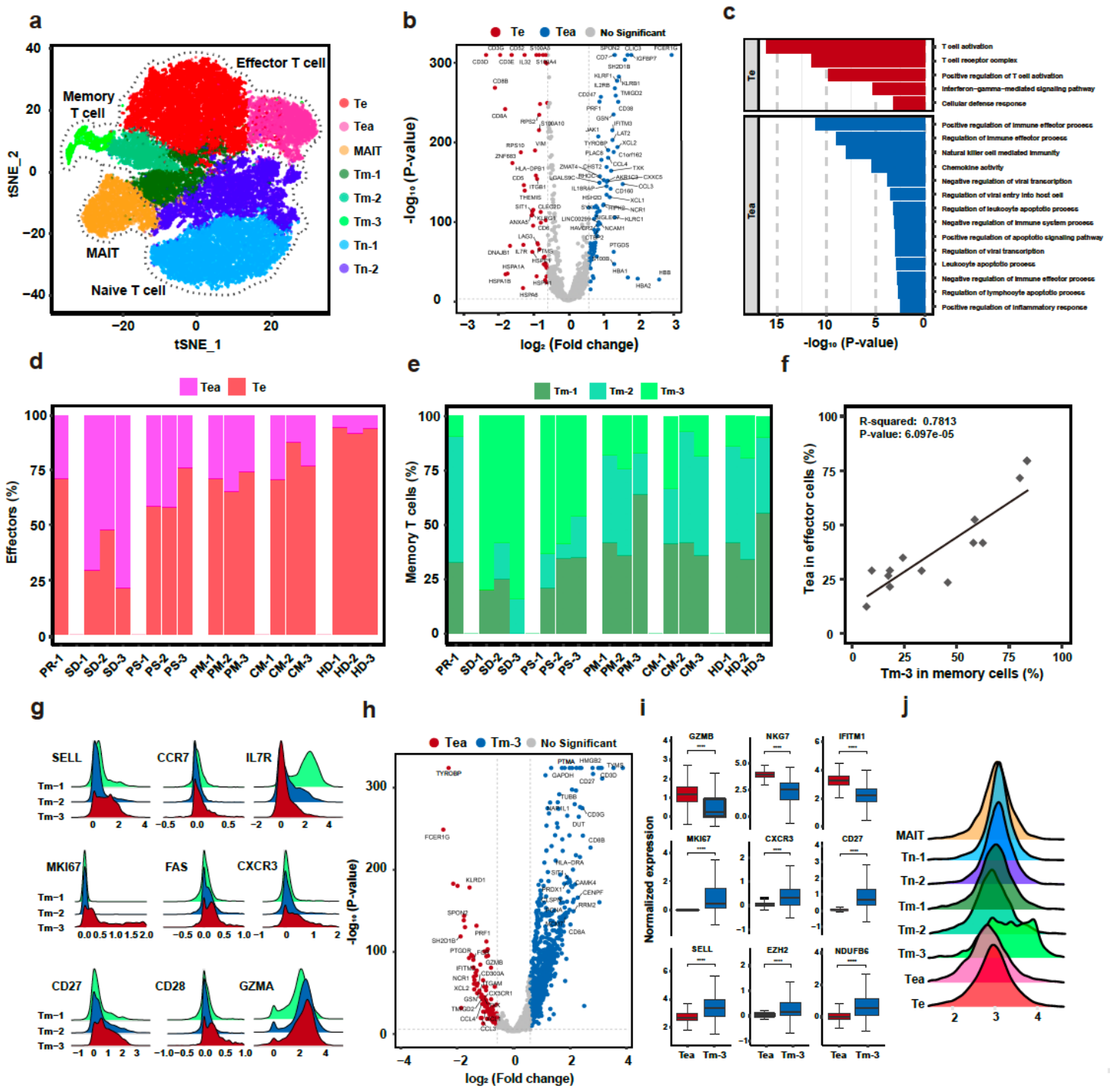

Figure 3

Excessive activation induced exhaustion of Tea cells. a. The t-SNE plot of CD8 T cells showing 8 clusters including Te, Tea, MAIT, Tm-1, Tm-2, Tm-3, Tn-1 and Tn-2. b. Volcano plot showing differentially expressed genes between Te and Tea cells. Red dots are representing significantly upregulated genes in Te cells compared to Tea cells and blue dots are representing significantly upregulated genes in Tea cells compared to Te cells (|log2(FC)|>0.58, P value<0.05). c. Gene Ontology (GO) enrichment analysis of significantly differentially expressed genes between Te and Tea cells. d. The proportion of the two different effector CD8 T cells (Tea and Te) in each patient. e. The proportion of the three different memory CD8 T cells (Tm-1, Tm-2 and Tm-3) in each patient. f. Scatter plot showing the correlation between proportions of Tea cells in effector cells and proportions of Tm-3 cells in memory cells. g. The ridgeline plot visualizing expression distributions of differentially expressed genes in Tm-1, Tm-2 and Tm-3 cells. h. Volcano plot showing differentially expressed genes between Tea and Tm-3 cells. Red dots are representing significantly upregulated genes in Tea cells compared to Tm-3 cells and blue dots are representing significantly upregulated genes in Tm-3 cells compared to Tea cells (|log2(FC)|>0.58, P value<0.05). i. Boxplots showing the selected differentially expressed genes between Tea and Tm-3 cells. i. The ridgeline plot visualizing expression distributions of Prothymosin Alpha (PTMA) gene in CD8 T cell subsets.

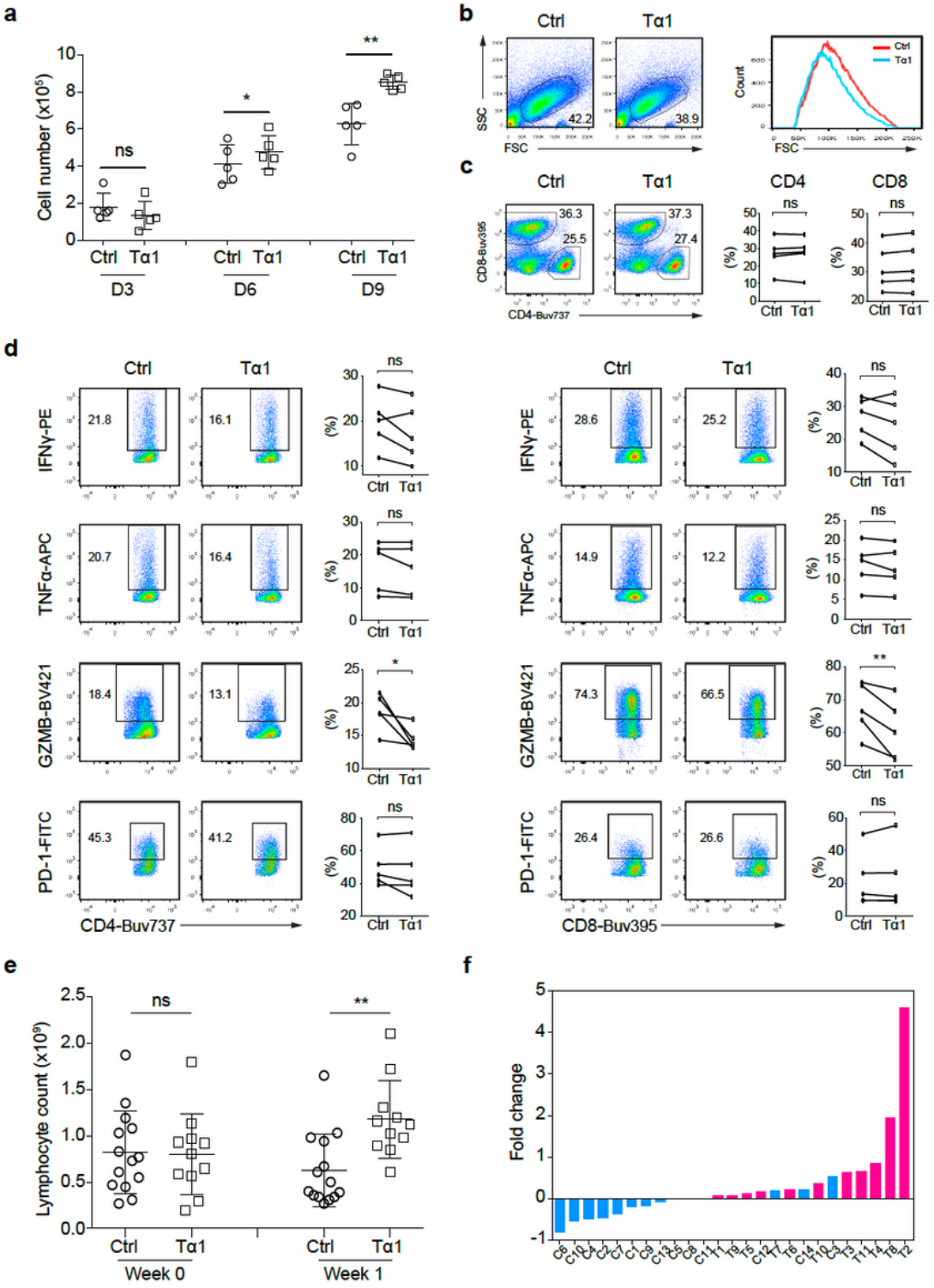

Figure 4

Thymosin α1 protected T cells from excessive activation. a. PBMCs were activated with CD3/CD28 (pre-coated) antibodies in the presence or absence of Tα1 (200ng/ml), cell numbers were counted on day 3, 6 and 9 post-activation respectively. Cells collected at day 3 were analyzed as indicated. b. Analysis of the cell size of activated PBMCs treated with Tα1. c. Analysis of the proportion of CD4 and CD8 T cells in activated PBMCs treated with Tα1. d. Paired analysis of activation markers in CD4 and CD8 T cells

treated with Tα1. Activated PBMCs were collected at day 3 and were stained with antibodies specific for IFNγ, TNF, Granzyme B and PD-1. e. Lymphocyte count was recorded in 25 SARS-CoV-2 patients treated with or without Tα1 at week 0 and 1. f. Fold change in lymphocyte count after 1 week of Tα1 treatment in 25 SARS-CoV-2 patients (Conventional therapy (Ctrl) n=14, Tα1 treatment n=11). For in vitro experiments (n=3 biological replicates, * p≤0.05, **p≤0.01).

Supplementary Files

This is a list of supplementary files associated with this preprint. Click to download.

- Supplementalfigures.pdf
- TableS1.xlsx